Determination of longitudinal profile of railway track using vehicle-based inertial readings

Eugene J. OBrien[1], Cathal Bowe[2], Paraic Quirke[1,2], Daniel Cantero[3]

[1]School of Civil Engineering, University College Dublin, Dublin 4, Ireland.
[2]Iarnród Éireann Irish Rail, Technical Department, Engineering & New Works, Inchicore, Dublin 8, Ireland.
[3]Department of Structural Engineering, Norwegian University of Science & Technology, Trondheim, Norway.

ABSTRACT: The longitudinal profile of a railway track excites a dynamic response in a train which can potentially be used to determine that profile. A method is proposed in this paper for the determination of the longitudinal profile through an analysis of bogie vertical accelerations and angular velocities resulting from the train/track dynamic interaction. The Cross Entropy optimisation technique is applied to determine the railway track profile elevations that generate a vehicle response which best fits the measured dynamic response of a railway carriage bogie. Numerical validation of the concept is achieved by using a 2-dimensional quarter-car dynamic model, representing a railway carriage and bogie, traversing an infinitely stiff profile. The concept is further tested by the introduction of a 2-dimensional car dynamic vehicle model and a 3-layer track model to infer the track profile in the longitudinal direction. Both interaction models are implemented in MATLAB. Various grades of track irregularity are generated which excite the vehicle inducing a dynamic response. Ten vertical elevations are found at a time which give a least square fit of theoretical to measured accelerations and angular velocity. In each time step, half of these elevations are retained and a new optimisation is used to determine the next ten elevations along the length of the track. The optimised elevations are collated to determine the overall longitudinal profile over a finite length of railway track.

KEY WORDS: Railway Track; Longitudinal Profile; Drive-by; Vehicle Track Interaction; Cross Entropy, Optimisation.

INTRODUCTION

Increased demand on railway networks is reducing the time available to carry out the inspections necessary to determine track condition. As a result, the collection of acceleration and other dynamic parameters from sensors mounted on in-service vehicles is becoming more desirable as a tool for monitoring the condition of railway track. Dynamic measurements have economic and performance advantages over optical measurements which have a tendency to perform poorly in dirty railway environments. The drive-by nature of this Continuous Track Monitoring (CTM) system has the potential to provide 'real time' feedback to railway infrastructure managers on the condition of their network. This makes possible the forecast of track defect development, verification of quality of repairs and the improvement of maintenance management.[1]Traditionally, railway infrastructure managers assess the condition of their network using a Track Recording Vehicle (TRV): a specialised, instrumented train which periodically collects geometric data of the railway track including track gauge, longitudinal profile, alignment, super elevation irregularity (cross level or can't) and twist. European Standard EN13848[2] defines the method of measurement of railway track using TRVs in Europe. The standard also defines the approach for evaluating track condition by means of various safety related limits associated with each of the parameters measured so that maintenance interventions can be planned. TRVs are the current preferred method of measurement for these parameters. However, these vehicles are expensive to run and may disrupt regular services during their operation. Using in-service vehicles to determine these parameters presents a potential saving for railway infrastructure managers.

Track longitudinal profile can be considered as a representation of the vertical profile of a track made up of consecutive measurements of longitudinal level as defined in EN13848.[2] Rails are represented individually, i.e. a separate longitudinal profile exists for each rail. Rail longitudinal profile is comprised of a combination of macro changes in track elevation in the longitudinal direction (e.g. track grades, vertical curves, etc.) and local rail irregularities. Rail irregularities are geometrical deviations from the ideal rail longitudinal profile.

Railway track longitudinal profile is an important indicator of serviceability condition. It is desirable to have perfectly level track profiles so that dynamic responses of the vehicle are minimised, thereby increasing passenger comfort, reducing wear on vehicle components and reducing power consumption. A reduction in vehicle dynamics also reduces the vehicle load on the track. Therefore keeping a good vertical longitudinal profile helps maintain overall track condition through a reduction in vehicle dynamic effects.[3] However, it is inevitable that track irregularities will occur for a number of reasons including rail head manufacturing defects, wear, impact from wheel flats, track settlement and poor maintenance.[4] It is the passage of the vehicle across the irregularities on the track profile that excites it and invokes a dynamic response.

In numerical studies track irregularities can be generated using stationary random processes described by Power Spectral Density (PSD) functions. PSD is used in several countries (including the US, Germany, China and France) to classify track quality according to its irregularity spectrum.[5] Definitions of PSD functions vary significantly due to their empirical nature and differences in measuring instruments and evaluation methods used in their formulation.[6] Perrin *et al.*[7] propose an alternative method for generating more realistic track geometry irregularities based on statistical properties of measured data. Recently, the possibility of using inertial methods to estimate track profiles using acceleration data measured on a vehicle has gained considerable interest. Weston *et al.*[8] provide a review of the state of the art of track monitoring using in-service vehicles. Most Unattended Geometry Measurement Systems (UGMS) fixed to in-service trains require both inertial and optical sensors to return the parameters required for full assessment of track geometry. A drawback of using UGMS is that the in-service vehicles hosting the systems are required to stop at stations more regularly than dedicated measuring trains. This has the effect of reducing the speed of the UGMS vehicles in certain areas, compromising accuracy of measurement. The use of accelerometers and rate gyroscopes on the bogie level of a railway vehicle to estimate a pseudo-track geometry has been investigated by Weston *et al.*[9] Real *et al.*[10] use frequency domain techniques to estimate track profile. A mixed acceleration data filtering approach is used by Lee *et al.*[11] in the measured acceleration for stable displacement estimation and waveband classification of the irregularities.

In this paper the Cross Entropy (CE) combinatorial optimisation method, as described by de Boer et al.[12], is adapted to determine track longitudinal profiles. Harris *et al.*[13] use the CE combinatorial optimisation technique to characterise vehicle model parameters and road surface profiles using measured vehicle acceleration responses. However, to the authors' knowledge, the CE method has not previously been used to determine longitudinal profiles for railway track. In this paper dynamic interaction models are used in favour of moving load models so that dynamic effects are not overestimated and more realistic acceleration histories can be generated.[14]

This paper reports the results of the numerical simulations carried out to test the concept of using CE optimisation to determine track longitudinal profile. The next section explains the numerical models used for the simulations. Following this, the CE method is described and the optimisation processes are discussed. This is followed by the results of the optimisation that validates the methodology for a range of profiles.

MODEL DESCRIPTION

Numerical simulation of the Vehicle-Track Interaction (VTI) is used in assessing the application of CE optimisation to the estimation of track longitudinal profile for given vehicle dynamic response. VTI calculations are carried out in Matlab[15] to generate the dynamic response of a vehicle travelling longitudinally along a track. The vehicle models, track model and PSD method for generating track irregularities are described in this section along with a brief description of the vehicle and track model coupling. Two levels of model complexity are used. The method is initially tested using Model A, a simple quarter-car vehicle model crossing a series of rigid rail profiles (i.e. deflection in the rail is not permitted). To demonstrate the capabilities of the algorithm, an inverted bell-shaped irregularity added to an otherwise level track profile. Three rail profiles featuring randomly generated irregularities with varying degrees of roughness are also generated and used in the numerical tests. In this model, irregularities represent variations from perfectly level track caused by deviation from design levels during construction, variation in track stiffness and from permanent deformation of track over time.

Following this, Model B, a relatively complex vehicle and 3-layer track model, is used to test the method. When coupled together, these models return more realistic vehicle accelerations, partly as a result of permitting the deflection of the track under load. Numerical validation of the method using Model B is carried out using three track profiles each featuring a different magnitude of track irregularity and one-track profile featuring both track irregularity and track settlement.

Model A: Quarter-Car on Infinitely Stiff Track

The quarter-car vehicle model used in this study, shown in Figure 1. Model A: quarter-car vehicle model on rail profile, is referred to as Model A. It consists of two masses; m_1 representing the quarter carriage mass and m_2 representing the suspension (bogie and wheelset) half mass. Each mass has a single degree of freedom (DOF), u_i, and they are connected by an elastic spring k_1 and damper c_1 representing the secondary suspension of the vehicle. The stiffness and damping of the bogie system are represented by k_2 and c_2 respectively that characterise the primary suspension of the vehicle. The sprung vehicle model is connected to the rail profile through its primary suspension system. This model is similar to vehicle descriptions used in other studies.[6]

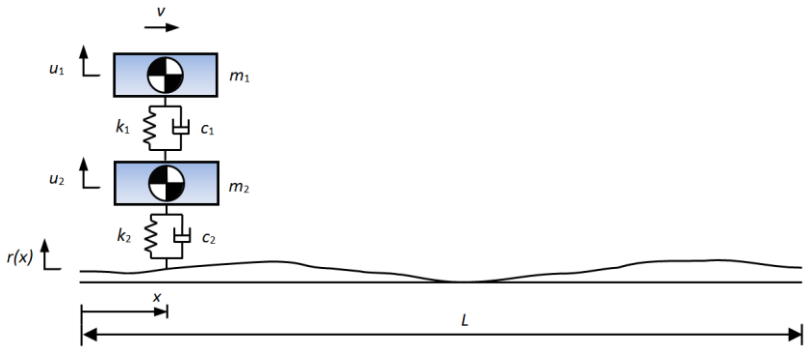

Figure 1. Model A: quarter-car vehicle model on rail profile

Table 1. Properties of Model A

Property	Unit	Symbol	Value
Mass of main body	kg	m_1	7 900
Mass of bogie and wheelset	kg	m_2	512.5
Damping of secondary suspension	Ns/m	c_1	15 000
Damping of primary suspension	Ns/m	c_2	5 000
Stiffness of secondary suspension	N/m	k_1	7.3×10^5
Stiffness of primary suspension	N/m	k_2	5×10^5

Model A is excited by irregularities on the track longitudinal profile while it travels at a constant speed, v. The vehicle response is then used to back-calculate the irregularities of the rail profile. The equations of motion of the vehicle model, expressed in the time domain, are as follows:

$$m_1\ddot{u}_1 + c_1(\dot{u}_1 - \dot{u}_2) + k_1(u_1 - u_2) = 0 \quad (1)$$

$$m_2\ddot{u}_2 - c_1\dot{u}_1 + (c_1 + c_2)\dot{u}_2 - k_1u_1 + (k_1 + k_2)u_2 = c_2r'v + k_2r \quad (2)$$

where r is the rail profile and r' is its first-time derivative with respect to distance. These equations can be represented in matrix form as follows:

$$\begin{bmatrix} m_1 & 0 \\ 0 & m_2 \end{bmatrix}\begin{Bmatrix} \ddot{u}_1 \\ \ddot{u}_2 \end{Bmatrix} + \begin{bmatrix} c_1 & -c_1 \\ -c_1 & c_1 + c_2 \end{bmatrix}\begin{Bmatrix} \dot{u}_1 \\ \dot{u}_2 \end{Bmatrix} + \begin{bmatrix} k_1 & -k_1 \\ -k_1 & k_1 + k_2 \end{bmatrix}\begin{Bmatrix} u_1 \\ u_2 \end{Bmatrix} = \begin{Bmatrix} 0 \\ c_2r'v + k_2r \end{Bmatrix} \quad (3)$$

i.e.,

$$\mathbf{M_v}\ddot{u}_v + \mathbf{C_v}\dot{u}_v + \mathbf{K_v}u_v = f_v \quad (4)$$

where $\mathbf{M_v}$, $\mathbf{C_v}$ and $\mathbf{K_v}$ are the mass, damping and stiffness matrices of the vehicle respectively. The vectors, $\ddot{u}_v$, $\dot{u}_v$ and u_v are the vehicle accelerations, velocities and displacements respectively.

The dynamic equations of motion of the system are solved using the Wilson-θ integration method[17,18] implemented in MATLAB. The value of the parameter, θ = 1.420815 is used for unconditional stability in the integration scheme.[19]

Model B: 2D Car Vehicle Model on 3-layer Track

Model B is a more elaborate vehicle-track model which is used in the second part of this paper. This model is developed from the train-track-bridge model described by Cantero *et al.*[20] In this section, the vehicle and track models are described separately before model coupling is briefly outlined.

2D Car Vehicle Model

The 2-dimensional car vehicle model used as part of Model B is shown in Figure 1. It consists of 10 DOFs including 4 wheelsets (vertical translation only), 2 bogies (vertical translation and rotation

about each centre of gravity) and the main body (vertical translation and rotation). The wheelsets are represented as masses (m_{w1}, m_{w2}, m_{w3}, m_{w4}). The bogies are modelled as rigid bars with mass (m_{b1}, m_{b2}) and moment of inertia (I_{b1}, I_{b2}), and the main body of the vehicle is modelled as a rigid bar with mass (m_v) and moment of inertia (I_v). The wheelsets are connected to the bogies by means of primary suspension systems consisting of springs (k_p) and viscous dampers (c_p) in parallel. Similarly, the bogies are connected to the main body by means of a secondary suspension system consisting of a spring (k_s) and a viscous damper (c_s) in parallel. Assuming small rotations, a linearized system of equations of motion, as per Model A, is adopted (equation (4)).[21] This vehicle configuration is used in many other studies.[22-24] Vehicle properties are gathered from the literature[25] and are listed in Table 2.

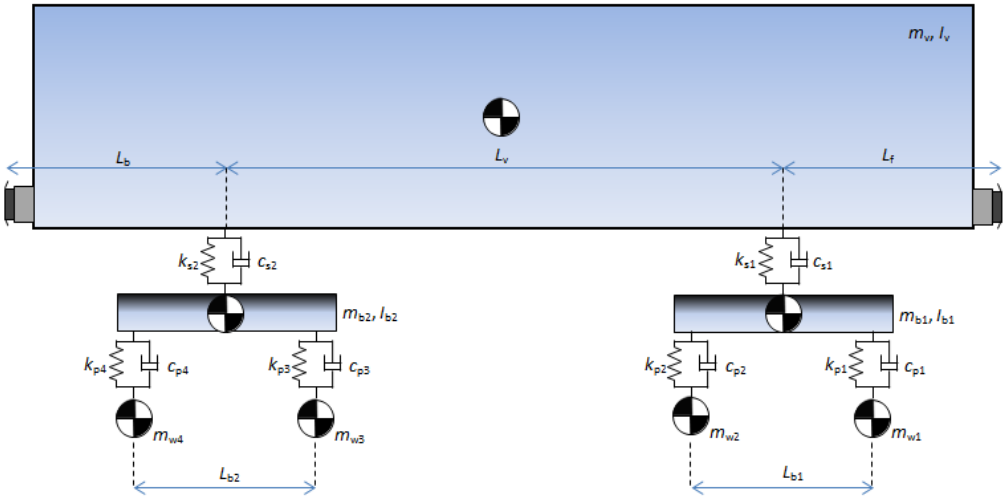

Figure 1. Model B: 2D car vehicle

Table 2. Mechanical properties of the 2D car vehicle (ICE3 Velaro)

Property	Unit	Symbol	Value
Mass of wheelset	kg	$m_{w1}, m_{w2}, m_{w3}, m_{w4}$	1 800
Mass of bogie	kg	m_{b1}, m_{b2}	3 500
Mass of main body	kg	m_v	47 800
Moment of inertia of bogie	kg.m^2	I_{b1}, I_{b2}	1 715
Moment of inertia of main body	kg.m^2	I_v	1.96×10^6
Stiffness of primary suspension	N/m	$k_{p1}, k_{p2}, k_{p3}, k_{p4}$	2.4×10^6
Stiffness of secondary suspension	N/m	k_{s1}, k_{s2}	0.7×10^6
Damping of primary suspension	Ns/m	$c_{p1}, c_{p2}, c_{p3}, c_{p4}$	20×10^3
Damping of secondary suspension	Ns/m	c_{s1}, c_{s2}	40×10^3
Distance between bogies	m	L_v	17.375
Additional distance (front and back)	m	L_b, L_f	3.7
Distance between axles	m	L_{b1}, L_{b2}	2.5

Track Model

A railway track is a 3D system exhibiting complex interactions between its constituent parts. Owing to this complexity there does not appear to be a definitive method to define model parameters to fully

characterise these interactions. In this paper, the track is modelled as a beam supported on a 3-layer sprung mass system representing a sleeper, pad and ballast support system as shown in Figure 2. This 3-layer track model is commonly used in the literature to define track behaviour.[21,26-29] The rail, sleepers and ballast are initially in static equilibrium: the rail is perfectly flat and the DOF of the sleepers and ballast are all at the same height. Track irregularities, representing deviations from perfectly level track, are added to the rail. Adding track irregularities has no effect on the vertical positions of the track DOFs. The irregularities affect the instantaneous vertical position of the wheels as they pass a particular section of track.

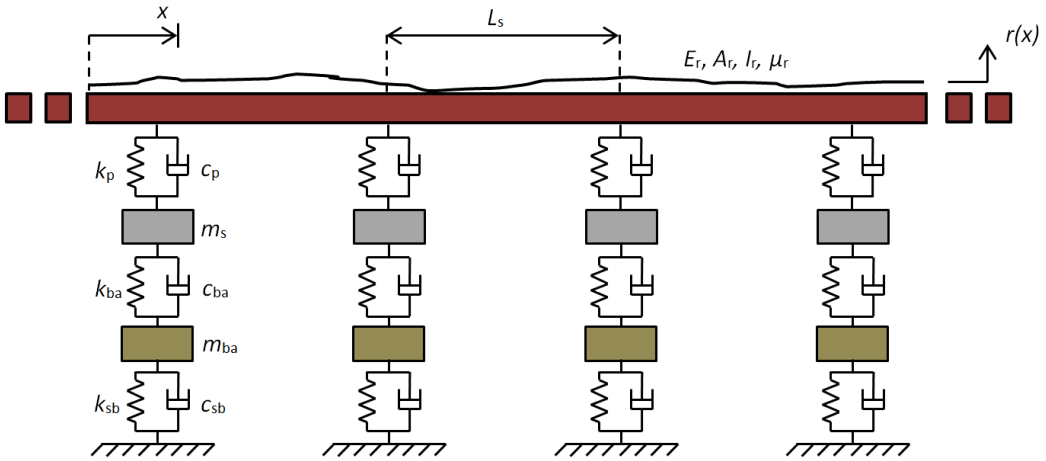

Figure 2. Model B: Track model

Track supports are spaced at a regular interval L_s, representing the spacing between the sleepers. The UIC60 rail is modelled as a finite element Euler-Bernoulli beam with one beam element per sleeper spacing. Each track element has 2 nodes with 2 DOFs at each node. Properties of track structures vary significantly throughout the literature. Values used in this study are taken from Zhai et al.27 and are shown in Table 3. A compilation of track model properties from a number of sources is listed in Cantero et al.20 The range of values cited indicate that track model parameters used in this paper appear to be in the middle range compared to values used by other authors.

Table 3. Properties of the track

Property	Unit	Symbol	Value
Elastic modulus of rail	N/m^2	E_r	2.059×10^{11}
Rail cross-sectional area	m^2	A_r	7.69×10^{-3}
Rail second moment of area	m^4	I_r	3.217×10^{-5}
Rail mass per unit length	kg/m	μ_r	60.64
Rail pad stiffness	N/m	k_p	6.5×10^{7}
Rail pad damping	Ns/m	c_p	7.5×10^{4}
Sleeper mass (half)	kg	m_s	125.5
Sleeper spacing	m	L_s	0.545
Ballast stiffness	N/m	k_{ba}	137.75×10^{6}
Ballast damping	Ns/m	c_{ba}	5.88×10^{4}
Ballast mass	kg	m_{ba}	531.4
Sub-ballast stiffness	N/m	k_{sb}	77.5×10^{6}

Sub-ballast damping	Ns/m	c_{sb}	3.115×10^4

The equation of motion for the track model can be defined by a set of second order differential equations:

$$\mathbf{M_t}\ddot{u}_t + \mathbf{C_t}\dot{u}_t + \mathbf{K_t}u_t = \mathbf{N_t}f_{int} \tag{5}$$

where $\mathbf{M_t}$, $\mathbf{C_t}$ and $\mathbf{K_t}$ are the mass, damping and stiffness matrices of the track respectively and $\ddot{u}_t$, $\dot{u}_t$ and u_t are vectors of track accelerations, velocities and displacements respectively. f_{int} contains the total interaction forces between the vehicle and the track at their contact points. $\mathbf{N_t}$ is a location matrix used to distribute the vehicle load to the DOFs of the rail and is calculated using Hermitian shape functions.[30,31]

Coupled Model

The vehicle and track subsystems are combined to form a coupled vehicle-track model. The coupling of the subsystems is expressed mathematically with additional off-diagonal block matrices as shown in equation (6):

$$\begin{pmatrix} M_V & 0 \\ 0 & M_T \end{pmatrix}\begin{Bmatrix} \ddot{u}_V \\ \ddot{u}_T \end{Bmatrix} + \begin{pmatrix} C_V & C_{V,T} \\ C_{T,V} & C_T \end{pmatrix}\begin{Bmatrix} \dot{u}_V \\ \dot{u}_T \end{Bmatrix} + \begin{pmatrix} K_V & K_{V,T} \\ K_{T,V} & K_T \end{pmatrix}\begin{Bmatrix} u_V \\ u_T \end{Bmatrix} = \begin{Bmatrix} F_V \\ F_T \end{Bmatrix} \tag{6}$$

or

$$\mathbf{M_g}\ddot{u} + \mathbf{C_g}\dot{u} + \mathbf{K_g}u = F \tag{7}$$

where $\mathbf{M_g}$, $\mathbf{C_g}$ and $\mathbf{K_g}$ are the global mass, damping and stiffness matrices respectively and F is the coupled system force vector. Subscripts V and T in equation (6) denote vehicle and track subsystems respectively.

The vehicle and track models are coupled via the wheel/rail interaction, i.e. the DOFs of the wheels and the DOFs of the rail are combined. At each time step, as the vehicle moves along the track, the coupled terms are updated. The vehicle wheels do not always act at the nodes of the rail and the contributions of the vehicle to the coupled terms need to be distributed to the DOFs of the rail using Hermitian shape functions.[23] It is assumed that the vehicle remains in contact with the rail at all times.

The equations of motion are solved using the Wilson- θ numerical integration scheme in MATLAB. A static analysis is carried out before a dynamic analysis is initiated. Furthermore, the vehicle is allowed to travel along the track for a minimum distance of 10 m so that vehicle dynamic equilibrium can be achieved before the measured accelerations are recorded. A time step of 0.002 s corresponding to a sensor scanning frequency of 500 Hz is used for the coupled model.

Track Profile and Irregularities

For this paper, three track profiles with random vertical irregularity are generated using the US Federal Railroad Administration (FRA) PSD function $S(\Omega)$ shown in equation (8).[32] The FRA function is chosen due to its common use in the literature.[22,33]

$$S(\Omega) = \frac{A_v\Omega_c^2}{(\Omega^2 + \Omega_r^2)(\Omega^2 + \Omega_c^2)} \tag{8}$$

where Ω is the spatial frequency, and coefficients A_v, Ω_r, Ω_c, relate to the grade of track and are given in Table 4. The three generated profiles, one of each line grade, and their associated PSDs, are illustrated in Figure 3.

Table 4. FRA American railway standard PSD coefficients

Line Grade	Quality	A_v	Ω_r [rad/s]	Ω_c [rad/s]
Class 4	Very Poor	2.39×10^{-5}	2.06×10^{-2}	0.825
Class 5	Poor	9.35×10^{-6}	2.06×10^{-2}	0.825
Class 6	Moderate	1.5×10^{-6}	2.06×10^{-2}	0.825

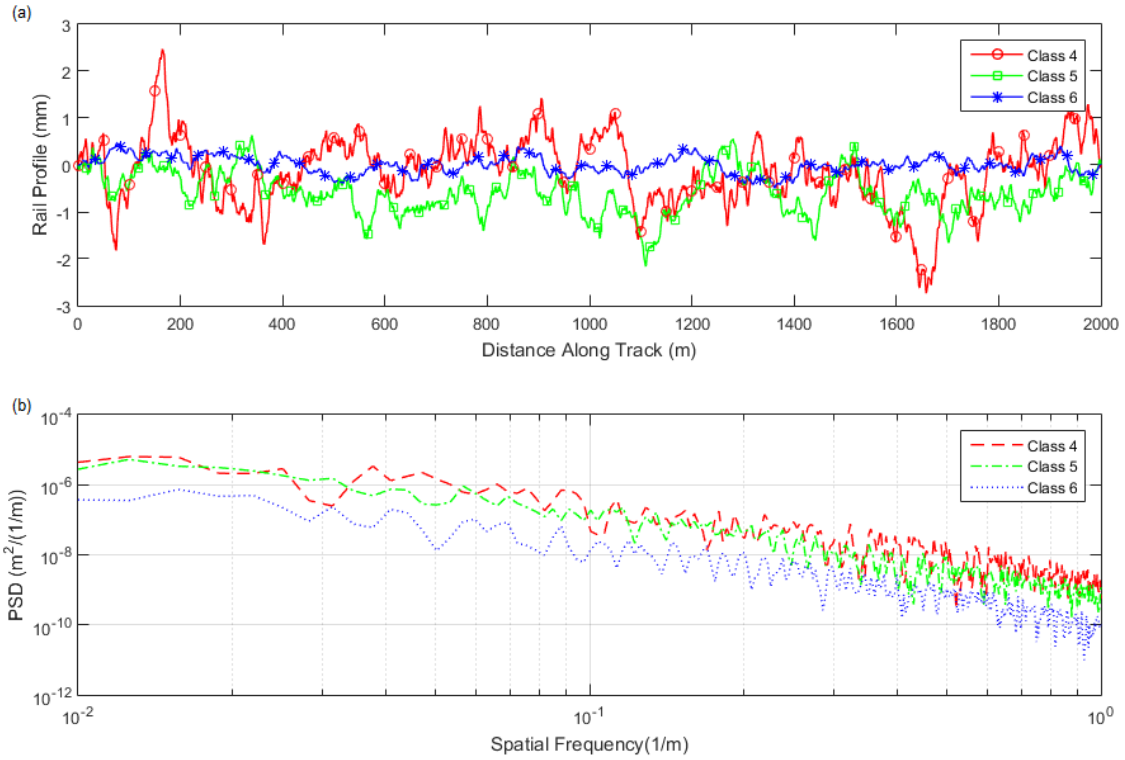

Figure 3. a) FRA track profiles; b) Power Spectral Densities (PSDs)

CROSS-ENTROPY METHOD

Cross-Entropy is a combinatorial optimisation technique used here to infer a series of track longitudinal profiles along a track from inertial measurements of the vehicle response. The CE method is an iterative procedure which firstly generates a population of trial solutions (a population of longitudinal profiles in this case) according to a specified random mechanism. An objective function, using the 1st generation of trial solutions, is applied to identify an 'elite set', a sub-set of the most optimal solutions. This elite set is then used to generate a new population. The process is repeated over many generations and converges to a global minimum (See Figure 4).[12] The method has been applied to a variety of Civil Engineering problems.[13,34-36]

In this study populations of track longitudinal profiles are generated and tested to determine which profiles produce vehicle responses most similar to the actual measured response, referred to here as the reference signals. The reference signals are taken from an initial VTI analysis before starting the optimisation technique. A VTI is then simulated for each profile in the population, returning signals for the DOFs being analysed to determine the objective function value for each profile in the population.

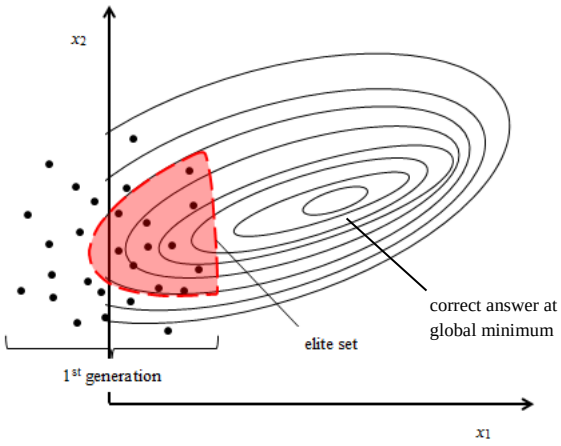

Figure 4. Cross Entropy method – Contours of objective function for 2-dimensional optimisation problem. Points represent trail solutions for the 1st generation

The initial population of profiles is generated through Monte Carlo simulation assuming a normal distribution defined by an initial mean and standard deviation for the first point in each of the profiles. Each subsequent point is generated by means of a random walk process, i.e. using the value of the previous point as the mean and the same initial standard deviation as shown in equation (9):

$$\begin{matrix} x_1 & x_2 & \cdots & x_m \\ \downarrow & \downarrow & \cdots & \downarrow \\ \mathcal{N}(\mu_i, {\sigma_i}^2) & \mathcal{N}(x_1, {\sigma_i}^2) & \cdots & \mathcal{N}(x_{m-1}, {\sigma_i}^2) \end{matrix} \tag{9}$$

where x is the elevation, m is the number of elevations in the profile, μ_i is the initial mean and σ_i is the initial standard deviation.

Objective Function

Two objective functions are tested in this paper. Both functions use a least squares fitting approach. The first objective function considers the entire signal while the alternative evaluates objective sub-functions for each value in the signal. The first objective function is used with Model A and tested for suitability with Model B, while the second objective function is used with Model B.

The first objective function, O, (equation (10)) is defined as the sum of the squared differences between vehicle accelerations calculated for a trial profile, $\ddot{u}_{trial,t}$, and the reference acceleration signal, $\ddot{u}_{ref,t}$:

$$O = \sum_{t=1}^{T} \left(\ddot{u}_{trial,t} - \ddot{u}_{ref,t}\right)^2 \tag{10}$$

where t is the scan number, and T is the total number of scans in the acceleration signal. The values of O for each trial profile in the population are ranked and an elite set of profiles identified. In this study, the elite set represents the best 10% of trial profiles. The procedure is illustrated in Figure 5.

The elite set is used to calculate the mean, μ_m and standard deviation, σ_m for each elevation in the profile. These means and standard deviations are used to generate an improved population of profile estimates for the next generation. This process is repeated until convergence is achieved (see section on convergence below).

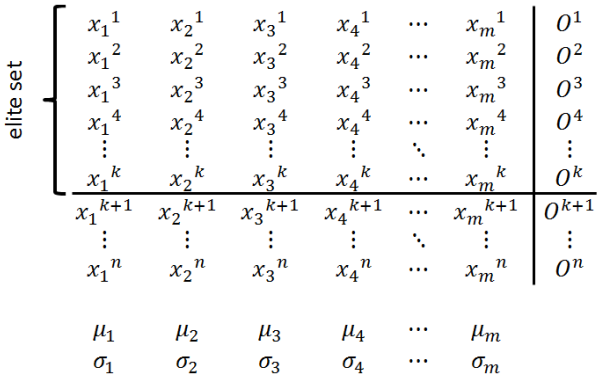

Figure 5. Cross Entropy method using a population of n profiles, each consisting of m elevations, x. The k lowest objective function values, O^1-O^k, represent an elite set of k profiles.

Using objective function O with Model B results in poor performance (see section on convergence below). An alternative approach to the calculation of the objective function consisting of objective sub-functions, O_t, is tested to resolve this issue. In the VTI, as a result of the time-space discretisation used, there exists a set of state vectors for each elevation in the track profile. In this method the t^{th} objective sub-function O_t, is calculated for each value of bogie vertical acceleration, $\ddot{u}$, and bogie angular velocity, $\dot{\theta}$, in the signal:

$$O_t = W_A\left(\ddot{u}_{trial,t} - \ddot{u}_{ref,t}\right)^2 + W_R\left(\dot{\theta}_{trial,t} - \dot{\theta}_{ref,t}\right) \tag{11}$$

where W_A is a weighting factor for the bogie acceleration and W_R is a weighting factor for the bogie angular velocity. Weighting factors are required due to differences in the power of the signals so that the signals' influence on the value of the objective sub-function can be equalised.

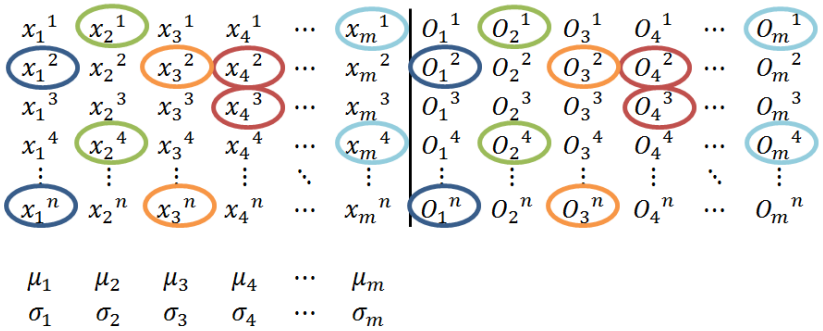

Figure 6. Alternative Cross Entropy method using a population of n profiles consisting of m elevations, x. The k lowest objective sub-function values O_t are used to gather an elite set of k estimates for each elevation in the profile represented here by the circled values. In this sample $k = 2$.

Weighting factors are calculated using the ratio of the root mean square values of the reference signals as follows:

W_A=〖RMS〗_R/(〖RMS〗_A+〖RMS〗_R) (12)

W_R=1- W_A (13)

where 〖RMS〗_A is the root mean square of the reference acceleration and 〖RMS〗_R is the root mean square of the reference angular velocity. The m objective sub-functions of each profile elevation in the population of n profiles are illustrated in Figure 7. In this version of CE objective sub-functions are ranked and used to find the elite set of elevations for each position in the profile. The elite set is used as before to calculate the mean, μ_m and standard deviation, σ_m for each elevation x_m, and used to generate an improved population of profile estimates for the next iteration. This approach is similar to that used by Dowling et al.35

Stepping through the profile

Depending on the sampling interval and length of the profile being inferred, there may be a large number of unknowns in the problem. This means that a very large population size would be required and there is a risk that the algorithm may not converge. To overcome this problem the optimisation is split into a number of phases. In this method, the phase location is represented by a 'window' of the profile. A number of unknowns, m, are determined within the window before moving to the next phase. At the end of each phase, the first $m/2$ best estimates of the profile elevations are saved as the estimated profile, and the remaining $m/2$ profile elevations are used as the first $m/2$ means for the next phase of m unknowns. To increase the efficiency of the algorithm, the remaining $m/2$ mean values for the next phase are taken as the m^{th} mean from the previous phase. Standard deviation is also reset to account for the relative uncertainty in profile elevations further along the phase window being analysed. This is achieved by increasing the standard deviation in an array from 0.1 in increments of $1/m$ to 1. A schematic of the phasing procedure used to determine long profiles is shown in Figure 7. The track distance covered by the phase window is a function of the number of profile elevations being inferred in each phase, vehicle speed and sensor scan rate. Stepping through the model in phases also reduces the size of the track model required in the interaction and therefore minimises the computational effort required.

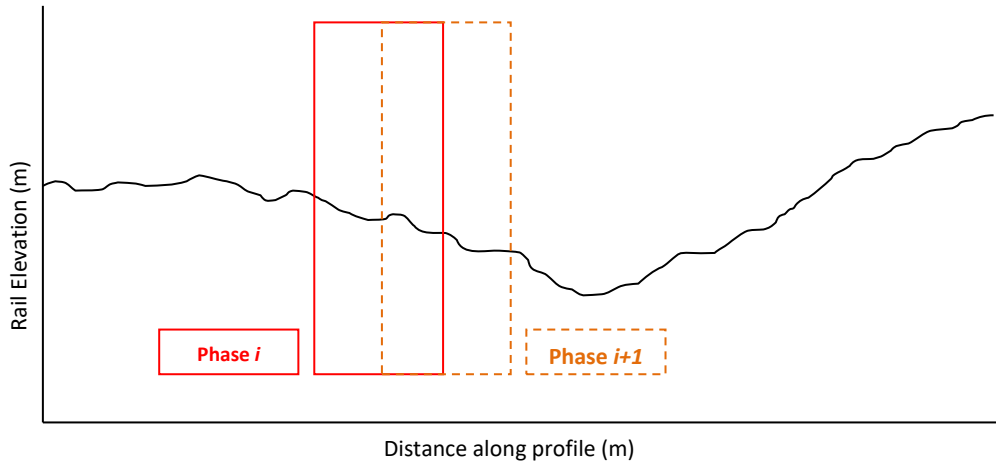

Figure 7. Stepping through track profile in phases

As stated in the section describing the coupled model, it is generally required to allow the vehicle to cross a minimum length of track so that vehicle dynamic equilibrium can be attained. To avoid this necessity during the stepping procedure and to ensure the acceleration and angular velocity signals generated can be compared to the reference signals, model vectors are transferred from an equivalent vehicle position in the previous phase. This ensures that the vehicle remains in dynamic equilibrium at the start of the phase. This method is also used by Quirke *et al*.[36]

Figure 8 shows the transfer of displacement, velocity and acceleration vectors required to maintain dynamic equilibrium in Model A. Since there is no track model in this interaction it is only necessary to transfer vehicle model vectors from the equivalent track position of the vehicle in the two phases: i.e. scan number $t = \tau$ in Phase i, to scan number $t = 1$ in Phase $i + 1$, where $\tau = T/2$.

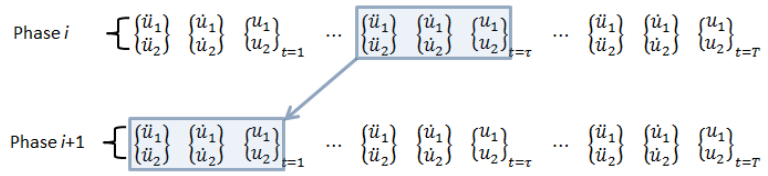

Figure 8. Transfer of model vectors for Model A

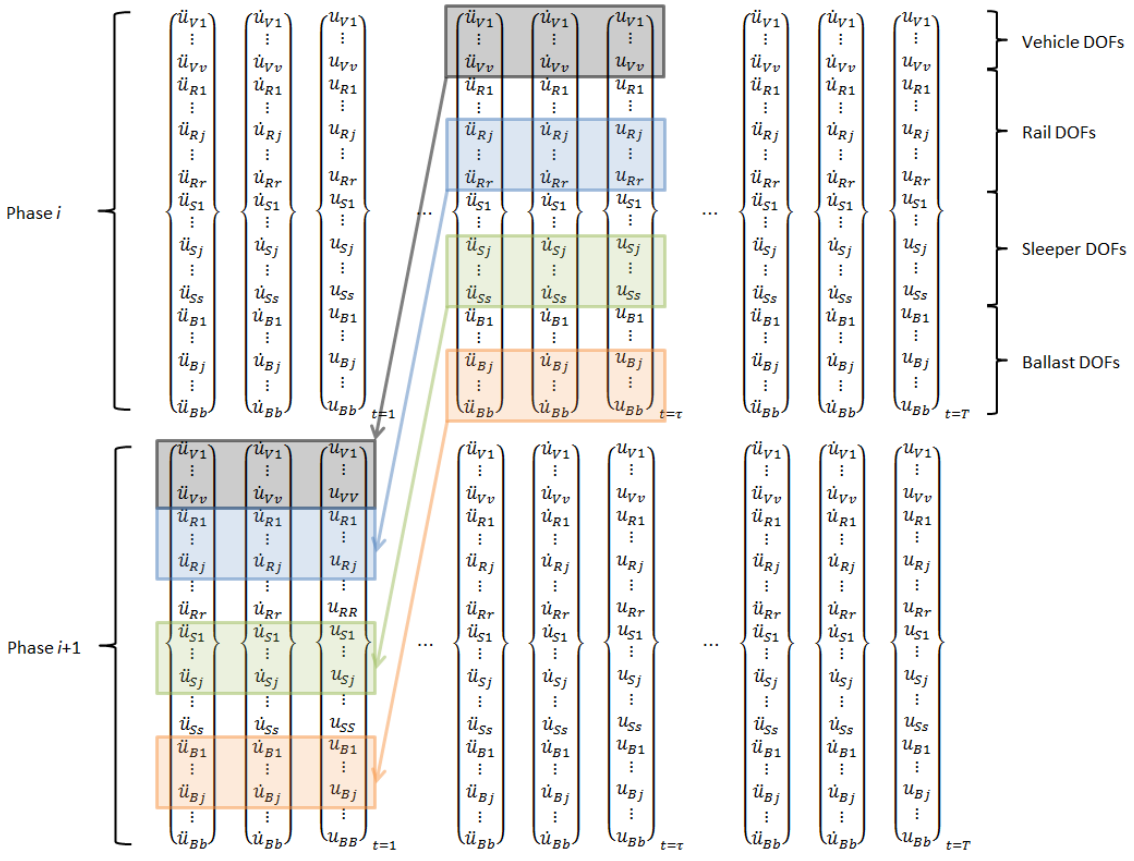

Figure 9. Transfer of state vectors for Model B. Shaded areas: Vehicle DOFs – subscript V; Rail DOFs – subscript R; sleeper DOFs – subscript S, ballast DOFs – subscript B

Figure 9 shows the transfer of the displacement, velocity and acceleration vectors required to maintain vehicle dynamic equilibrium in Model B. In this model, there are a total of v vehicle DOFs denoted with subscript V, r rail DOFs (subscript R), s sleeper DOFs (subscript S), and b ballast DOFs (subscript B). All vectors associated with the vehicle DOFs are transferred between phases. Due to

high bending stiffness in the rail, the effect of the vehicle load is distributed along the track.[37] Therefore the vectors defining translations and rotations in the rail, sleeper and ballast nodes for the track model section that is significantly affected by the vehicle load must be transferred. The vector groups are identified (from DOFs denoted by the subscript j to the DOF at end of the track layer) and transferred from the time $t = \tau$ in Phase i, to time $t = 1$ in Phase $i + 1$, the equivalent track position of the vehicle in the two phases. This method maintains vehicle and track equilibrium and minimises the size of the track model for computational efficiency.

Convergence

The CE optimisation requires a convergence criterion so that the iterative process is terminated once a solution has been found within a phase. Further to this, the solution is checked by restarting the optimisation until two similar solutions are found consecutively. Convergence of the optimisation within a phase is said to be achieved once the sum of the squared differences between the means of the elevation values, known as a convergence value, falls below a convergence threshold chosen according to the accuracy desired. The process is restarted using elevations of the profile inferred in the previous optimisation as the mean values for the first generation of profiles in the next optimisation for the phase. This process continues until the elevation values of the inferred profiles between consecutive optimisations are within a certain percentage of each other. A percentage of 5% is used for this paper.

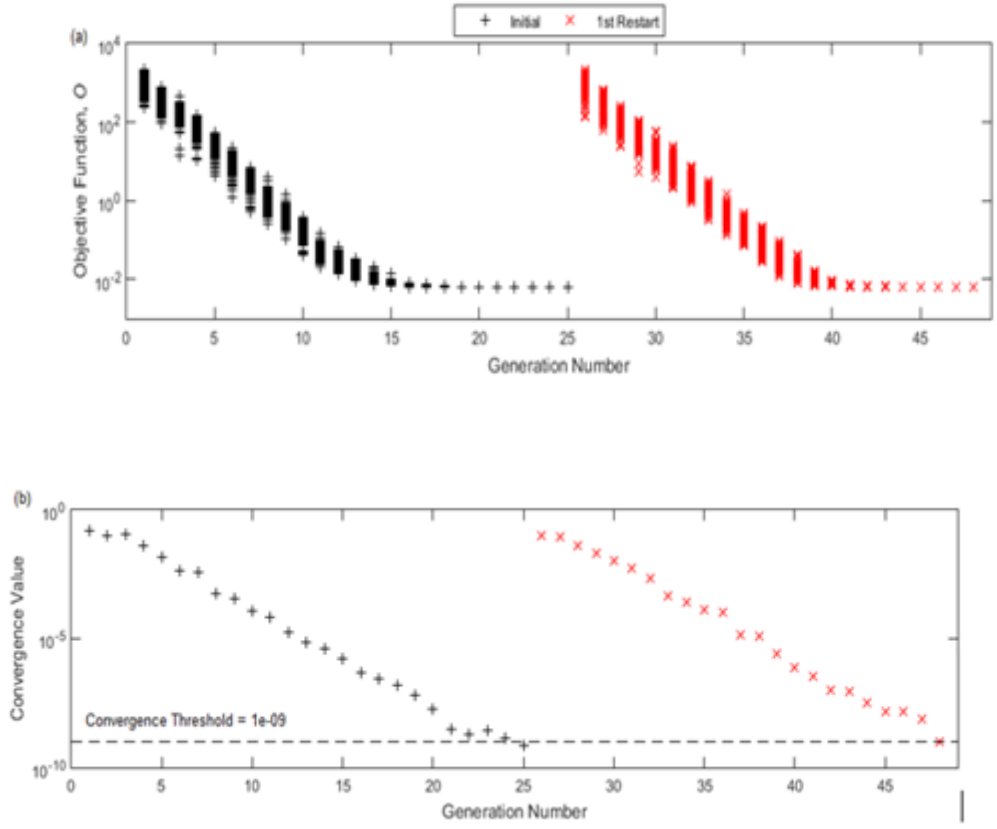

Figure 10. Performance of objective function *O* with Model A a) Objective function value, *O* vs. generation number for a phase with one restart; b) Convergence value (sum of squared differences between consecutive means) vs. generation number for the same phase

Figure 10a show the variation of objective function O using Model A for a phase with a population of 100 and an elite set size of 10. In the initial optimisation the method converges to a solution below the convergence threshold after 25 generations. The optimisation is restarted and converges to a similar solution in 23 generations. Only one restart is necessary for this example. The path of the convergence value is shown in Figure 10b. It can be seen that the algorithm restarts or terminates once the convergence value falls below the convergence threshold value. The total time take for this phase is 2.98 s, an average of 0.062 s per generation.

The performance of optimisation function O with Model B is shown in Figure 11. A lower threshold value is required to allow the optimisation to converge to a solution. The initial optimisation converges to a solution below the convergence threshold after 31 generations. The optimisation is restarted and converges to a similar solution in 20 generations. The total time taken for this phase is 127 s, an average of 2.49 s per generation.

The performance of the alternative optimisation sub-function O_t with Model B is shown in Figure 12. It can be seen that performance is greatly improved with the initial optimisation converging to a solution after 13 generations. The restarted optimisation also converges to a solution in 13 generations. The total time taken for this phase is 65 s, an average of 2.51 s per generation. Convergence of the optimisation sub-function method occurs in approximately half the time. This can be attributed to the lower dimensionality of the method, i.e. the number of variables contributing to the sub-function value.

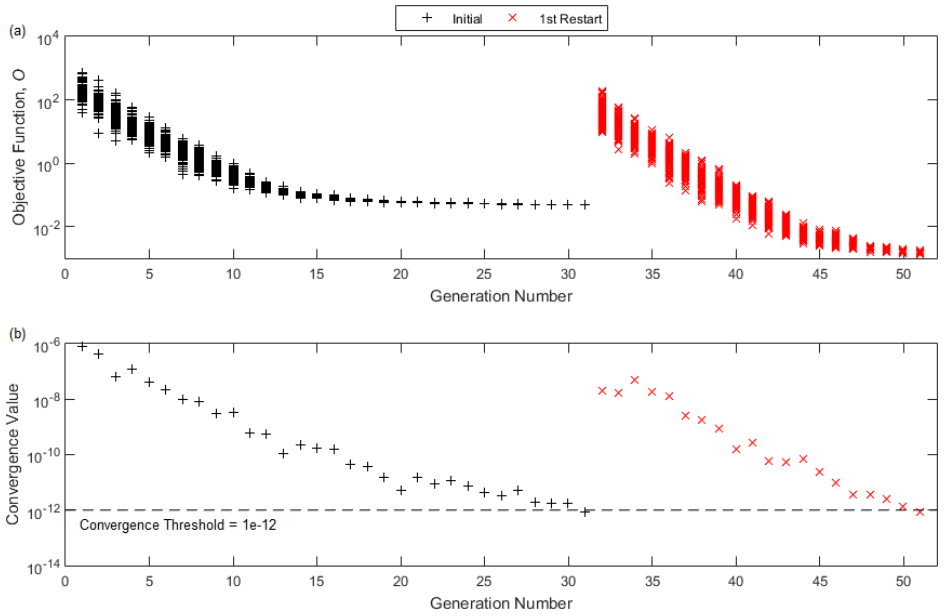

Figure 11. Performance of objective function *O* with Model B a) Objective function value, *O* vs. generation number for a phase with one restart; b) Convergence value (sum of squared differences between consecutive means) vs. generation number for the same phase

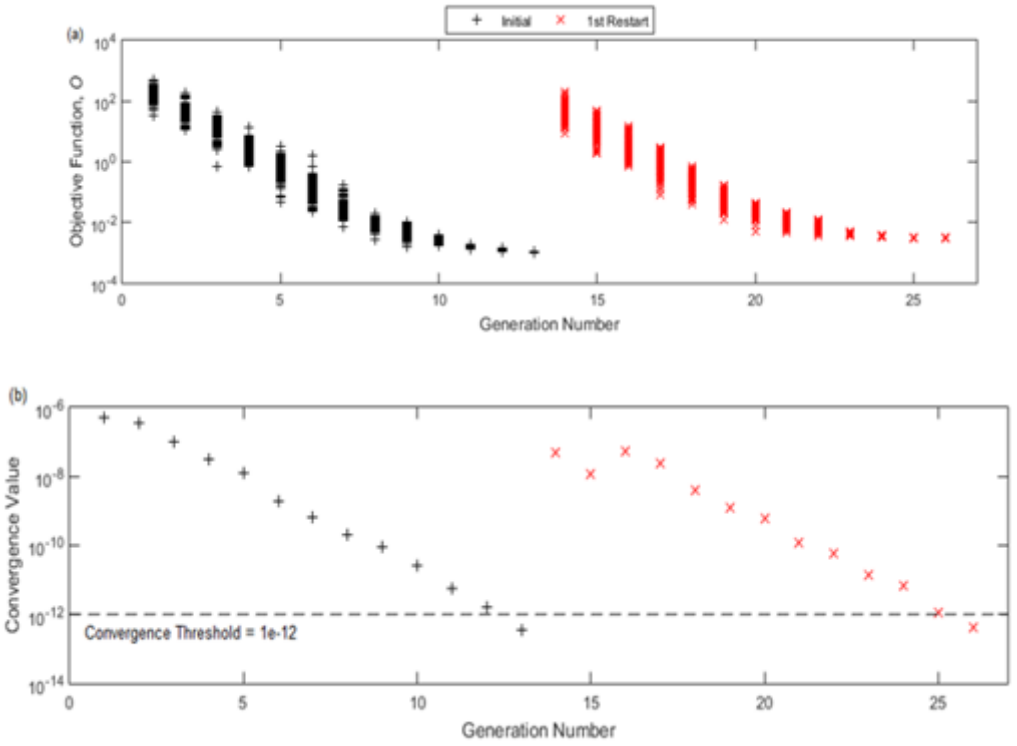

Figure 12. Performance of objective sub-function O_t with Model B a) Objective function value, O (sum of O_t) vs. generation number for a phase with one restart; b) Convergence value (sum of squared differences between consecutive means) vs. generation number for the same phase

RESULTS AND DISCUSSION

The results of a number of numerical tests of the CE method for determining track profiles are presented in this section.

Model A: Test Profile

A test profile is first used to demonstrate the capabilities of the method. This profile, shown in Figure 13a, is 20 m in length, and features an inverted 'bell' shaped variation along an otherwise perfectly level profile. The bell shape is defined using the equation of the normal statistical distribution, scaled by a factor. This irregularity, is located at 5.0 m, has a maximum depth of 0.002 m and a width corresponding to the standard deviation parameter of 0.5 (approximately 3.0 m). Using Model A, the quarter-car vehicle travels longitudinally over the rail profile at a constant velocity, v, of 108 km/h (30 m/s) generating the reference acceleration response of Figure 13b. Following this, the CE method, using objective function O, is executed using the parameters presented in Table 5. The acceleration signal from the vehicle bogie, m_2 is used as the reference acceleration.

Table 5. Cross Entropy optimisation parameters – Model A

Property	Value
Length of profile inferred per phase	0.25m
Number of elevation unknowns in each profile	10
Initial mean	0
Initial standard deviation	0.5mm
Size of each population of estimates	150
Size of elite set (percentage of population of estimates)	10%
Convergence threshold	1e-9

The inferred rail profile is shown in Figure 13a. An excellent estimate is found with small errors: in the region of ~0.018 mm. The computational time required to infer a profile 20 m in length was about 900 s using a 2.67 GHz processor and 6.0 GB RAM. This gives a rate of inference of approximately 45 s/m.

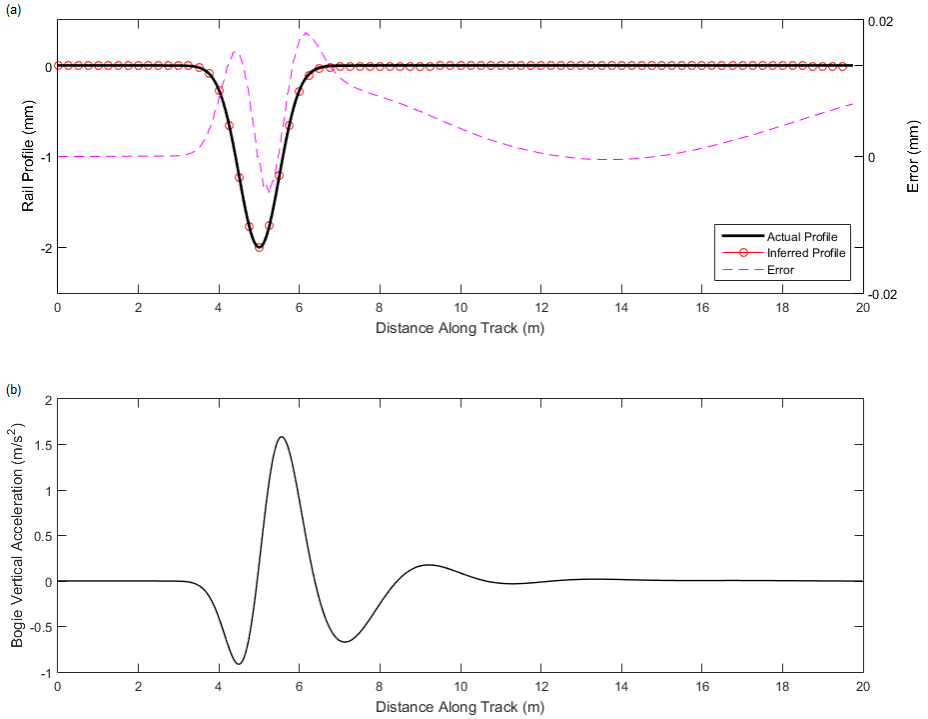

Figure 13. Model A: test profile. a) Quarter-car model estimation of perfectly level rail profile featuring an inverted 'bell'-shaped variation in the rail longitudinal profile; b) Bogie acceleration signal from VTI analysis

Model A: FRA Rail Profiles

For sections of the three FRA profiles shown in Figure 3, the quarter-car vehicle is modelled travelling at a constant velocity, v, of 108 km/h (30 m/s) to generate the reference acceleration responses. The increase in the number of irregularities and rate of elevation changes exhibited in the FRA profiles excite the vehicle in a more random fashion resulting in more realistic acceleration data. The same optimisation parameters presented in Table 5 are used with the method inferring the profiles at a similar rate to the test profile. Excellent estimates for all three profiles can be seen in Figure 14.

It is observed that there is a gradual drift in the estimated rail profile error, increasing with distance from the origin. Harris et al.13 found a similar drift when using road vehicle response to estimate road profiles and attributed this drift to an unavoidable accumulation of error due to double integration of measured acceleration. In addition, the amplitude of accelerations due to variations in profile for longer wavelengths is small and accelerometers are subject to larger magnitudes of noise at low frequencies. This means the sensor is unable to accurately measure low frequency changes in longitudinal profile thereby contributing to the drift. Indeed, as a constant slope does not generate any acceleration, it is not possible to use accelerations to detect that the carriage is on a constant slope unless the initial conditions are perfectly known. This error is not considered by the authors to be a problem as railway owners and managers are more interested in local variations in profile, rather than absolute deviations of the track.

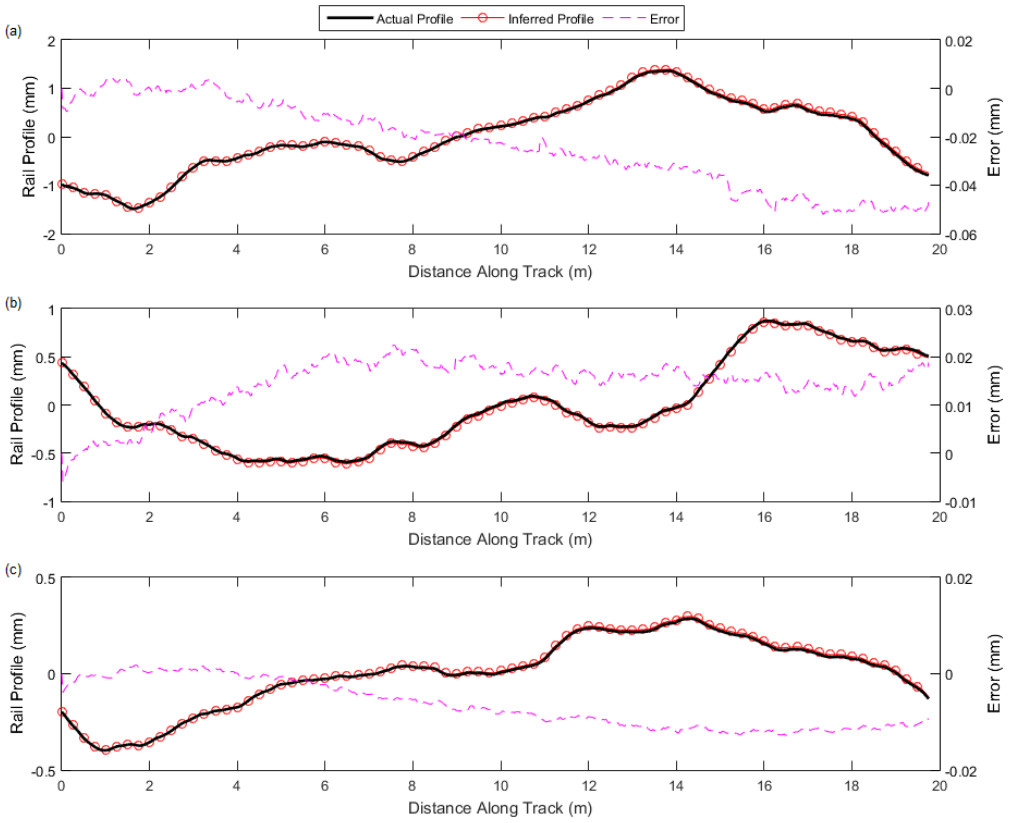

Figure 14. Model A: Inferred rail profiles and error a) FRA Class 4 Profile; b) FRA Class 5 Profile; c) FRA Class 6 Profile

Model B: FRA Track Profiles

This section presents the results from using Model B at a speed of 150 km/h (41.6 m/s) to infer sections of the three FRA track profiles of Figure 3. The CE method is executed using the objective sub-function O_t and optimisation parameters presented in

Table 6. The reference acceleration response is measured at the leading bogie vertical DOF of the 2D car while the reference angular velocity is measured at the leading bogie rotational DOF. Varying levels of sensor noise are added to the reference signals to test the resilience of the method to measurement noise. Sensor noise spectra for a range of accelerometers and a gyroscope are shown in Figure 15 and Figure 16 respectively.

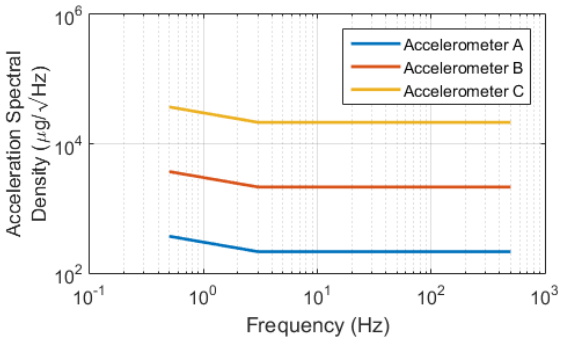

Figure 15. Accelerometer Power Spectral Density

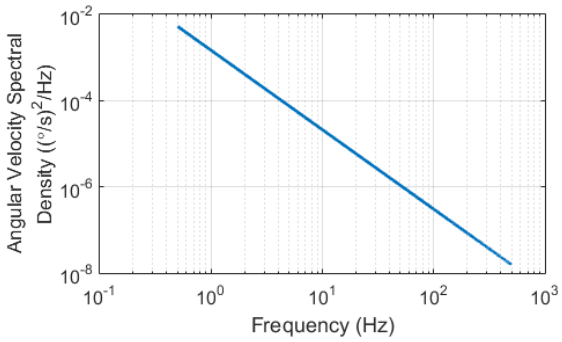

Figure 16. Gyroscope Power Spectral Density

Table 6. Cross Entropy optimisation parameters – Model B

Property	Value
Length of profile inferred per phase	0.833m
Number of elevation unknowns in each profile	10
Initial mean	0
Initial standard deviation	1mm
Size of each population of estimates	100
Size of elite set (percentage of population of estimates)	10%
Convergence threshold	5e-11

The results are presented in Figure 18. As noted above, there is an observable drift in the inferred profile from the actual profile which is, in this case, amplified by adding greater magnitudes of sensor noise to the reference signals. There appears to be issues with stability when using larger levels of sensor noise over better-quality track. This can be clearly observed in Figure 18c where the variation in the Class 6 track longitudinal profile is low resulting in small amplitudes in the reference signals characterising vehicle response. Added sensor noise dominates the signals and adversely affects the inference of longitudinal profiles using the method

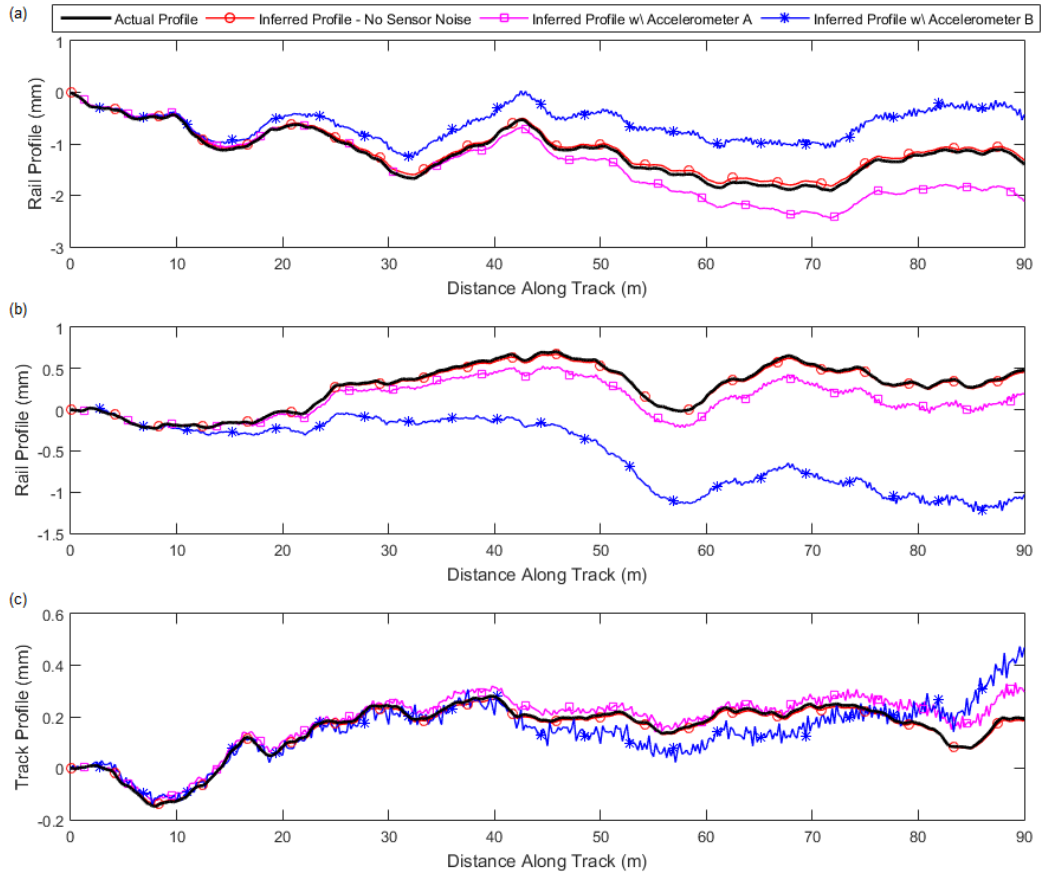

Figure 17. Model B: Inferred track profiles and effect of added sensor noise a) FRA Class 4 Profile; b) FRA Class 5 Profile; c) FRA Class 6 Profile

Model B: Track Profile with Elevation Change and FRA Irregularities

This section presents the results from using Model B, again at a vehicle velocity of 150 km/h, to infer a section of track exhibiting a large variation in elevation and FRA Class 4 track irregularities. This profile might be found along a section of track which is undergoing settlement. The profile, shown in Figure 18, is 120 m in length, and features an inverted 'bell' shaped variation in elevation with FRA Class 4 irregularity superimposed. The inverted bell is located at 100.0 m, has a maximum depth of 40 mm and a width corresponding to the standard deviation parameter of 10 (approximately 140.0 m). The optimisation is executed using objective sub-function O_t, and the parameters presented in

Table 6. Sensor noise generated using PSDs for Accelerometer C and the gyroscope shown in Figure 15 and Figure 16 are added to the reference signals prior to initiation of the optimisation.

The result shown in Figure 19 confirms that the method can detect, with reasonable accuracy, larger changes in elevation along a track. This demonstrates that it has the potential to be used to detect track settlement.

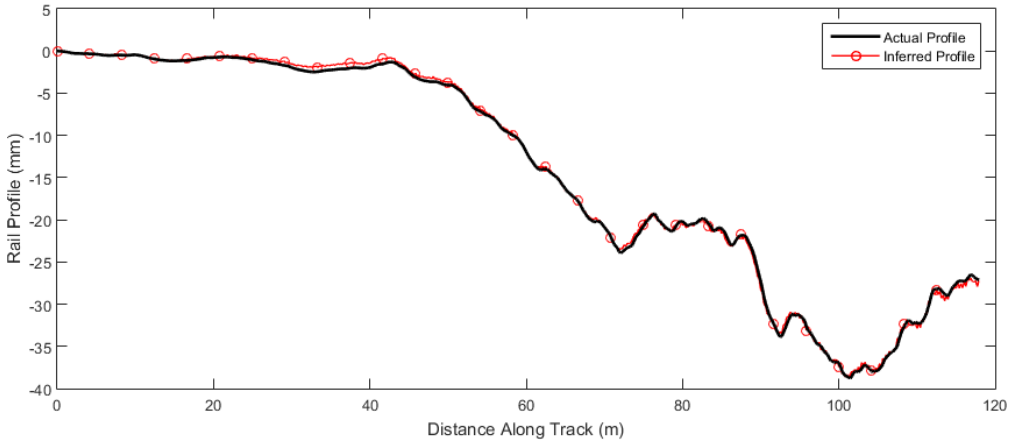

Figure 18. Model B: estimation of 40mm settlement in track with FRA Class 4 track Irregularities

SUMMARY AND CONCLUSIONS

A method for estimating railway longitudinal profiles using the Cross Entropy combinatorial optimisation method is presented in this paper. The analysis is carried out using acceleration signals generated from simplified railway vehicle and track models to infer the longitudinal track profiles. It is found that the estimated track profiles produced by the method provide a very good fit to the actual profiles and the method exhibits some resilience to added noise in the reference signals. Both track irregularities and larger scale changes in track elevation are successfully inferred.

The optimisation method uses idealised 2-dimensional multi-body vehicle and track models to compare to a reference signal. In this paper, the same model is used in the generation of both the reference signal and in the optimisation process which could be considered a shortcoming of the study. This greatly simplifies the problem in comparison to a situation where the reference signal is taken from field measurements. Future work on this topic should consider model inputs generated from alternative vehicle track interaction models or real-world measurements.

For this method to be employed to determine track profiles using acceleration data measured from an in-service train, accurate knowledge of vehicle and track properties is required. The accurate estimation of these parameters remains a challenge.[38] In addition, due to the simplistic nature of the track and vehicle models and idealised assumptions of a constant subgrade stiffness profile below the track structure, it can be said that the profile inferred from this method in a real situation is unlikely to be an exact match to the real profile. However, the purpose of this research is to identify locations on the track where maintenance is required. The hypothesis is that local reductions in stiffness as well as permanent deformation of track will result in local drops in the inferred profile. Furthermore, over time, if damage or track settlement occurs, these changes in the track profile will be reflected as changes in the inferred profile, making it possible to identify particular track sections as being damaged. Improvement in the accuracy of inferred profiles may be achievable through consideration of subgrade stiffness variation however this would require the inclusion of additional variables into the optimisation problem.

It is hypothesised that the variation of optimisation parameters such as population size and convergence criteria can be further optimised to achieve the desired balance of accuracy and efficiency in returning profiles at regular periods to inform maintenance planning. Reported track profile return rates of over 100 s/m (~800 m/day) are currently too slow for the method to be considered for real-time monitoring of an entire network. It is anticipated that improvements in algorithm efficiency and the use of more powerful parallel processors will improve on current computational time. In lieu of real-time application, the method has the potential to be used to determine track profiles periodically, on a more regular basis, and as compliment to, data gathered using dedicated track recording vehicles. The technique could be used to infer longitudinal profiles for localised track sections with known maintenance issues which require more regular monitoring.

From the results shown in this paper, it can be concluded that the Cross-Entropy method has the potential to be used as a ‘drive-by’ track monitoring tool to estimate and classify track profiles using relatively low-cost accelerometers fixed to trains in regular service. Accurate estimation of railway tracks longitudinal profile using sensors mounted on in-service vehicles has the potential to provide a valuable tool to inform maintenance planning and, through comparisons with past profiles, identification of track issues such as settlement.

ACKNOWLEDGEMENT

The research presented in this paper was carried out as part of the Marie Curie Initial Training Network (ITN) action FP7-PEOPLE-2013-ITN.The project has received funding from the European Union's Seventh Framework Programme for research, technological development and demonstration under grant agreement number 607524. The authors are thankful for this support.

REFERENCES

1. Nielsen J, Berggren E, Lolgen T, et al. *Overview of Methods for Measurement of Track Irregularities Important for Ground-Borne Vibration*. 2013.
2. IS EN 13848: Railway Applications - Track - Track Geometry Quality - CEN European Committee for Standardisation.
3. Frohling RD. *Deterioration of railway track due to dynamic vehicle loading and spatially varying track stiffness*. Ph.D. Thesis, University of Pretoria, South Africa, 1997.
4. Iwnicki SD. *Handbook of railway vehicle dynamics*. Taylor & Francis, 2006.
5. Berawi AR. *Improving railway track maintenance using power spectral density*. 2013.

6. Frýba L. *Dynamics of railway bridges*. London: Thomas Telford, 1996.
7. Perrin G, Soize C, Duhamel D, et al. Track irregularities stochastic modeling. *Probabilistic Eng Mech* 2013; 34: 123–130.
8. Weston P, Roberts C, Yeo G, et al. Perspectives on railway track geometry condition monitoring from in-service railway vehicles. *Veh Syst Dyn Int J Veh Mech Mobil* 2015; 53: 1063–1091.
9. Weston PF, Ling CS, Roberts C, et al. Monitoring vertical track irregularity from in-service railway vehicles. *Proc Inst Mech Eng Part F J Rail Rapid Transit* 2007; 221: 75–88.
10. Real J, Salvador P, Montalban L, et al. Determination of Rail Vertical Profile through Inertial Methods. *Proc Inst Mech Eng Part F J Rail Rapid Transit* 2011; 225: 14–23.
11. Lee JS, Choi S, Kim SS, et al. A mixed filtering approach for track condition monitoring using accelerometers on the axle box and bogie. *IEEE Trans Instrum Meas* 2012; 61: 749–758.
12. de Boer PT, Kroese D, Mannor S, et al. A tutorial on the cross-entropy method. *Ann Oper Res* 2005; 134: 19–67.
13. Harris NK, González A, OBrien EJ, et al. Characterisation of pavement profile heights using accelerometer readings and a combinatorial optimisation technique. *J Sound Vib* 2010; 329: 497–508.
14. Doménech A, Museros P, Martínez-Rodrigo MD. Influence of the vehicle model on the prediction of the maximum bending response of simply-supported bridges under high-speed railway traffic. *Eng Struct* 2014; 72: 123–139.
15. MathWorks. Matlab, Retrieved from http://www.mathworks.com/ (2016).
16. Cantero D, Basu B. Railway infrastructure damage detection using wavelet transformed acceleration reponse of traversing vehicle. *Struct Control Heal Monit* 2015; 22: 62–70.
17. Bathe KJ, Wilson EL. *Numerical methods in finite element analysis*. Englewood Cliffs, UK: Prentice Hall, 1976.
18. Tedesco JW, McDougal WG, Ross CA. *Structural dynamics, theory and applications*. California, USA: Addison Wesley Longman, 1999.
19. Weaver W, Johnston PR. *Structural dynamics by finite elements*. Indiana, USA: Prentice Hall, 1987.
20. Cantero D, Arvidsson T, OBrien E, et al. Train–track–bridge modelling and review of parameters. *Struct Infrastruct Eng* 2015; 2479: 1–14.
21. Nguyen K, Goicolea JM, Galbadon F. Comparison of dynamic effects of high-speed traffic load on ballasted track using simplified two-dimensional and full three-dimensional model. *Proc Inst Mech Eng Part F J Rail Rapid Transit* 2014; 228: 128–142.
22. Lei X, Noda N-A. Analyses of dynamic response of vehicle and track coupling system with random irregularity of track vertical profile. *J Sound Vib* 2002; 258: 147–165.
23. Lou P. Finite element analysis for train–track–bridge interaction system. *Arch Appl Mech* 2007; 77: 707–728.
24. Sun YQ, Dhanasekar M. A dynamic model for the vertical interaction of the rail track and wagon system. *Int J Solids Struct* 2002; 39: 1337–1359.
25. Goicolea JM. *Simplified Mechanical Description of AEV S-103 - ICE3 Velaro E High Speed*

Train. 2014.

26. Zhai WM, Wang KY, Lin JH. Two simple fast integration methods for large-scale dynamic problems in engineering. *Int J Numer Methods Eng* 1996; 39: 4199–4214.
27. Zhai WM, Wang KY, Lin JH. Modelling and experiment of railway ballast vibrations. *J Sound Vib* 2004; 270: 673–683.
28. Lu F, Kennedy D, Williams FW, et al. Symplectic analysis of vertical random vibration for coupled vehicle-track systems. *J Sound Vib* 2008; 317: 236–249.
29. Lei X, Zhang B. Influence of track stiffness distribution on vehicle and track interactions in track transition. *Proc Inst Mech Eng Part F J Rail Rapid Transit* 2010; 224: 592–604.
30. Fish J, Belytschko T. *A First Course in Finite Elements*. London: John Wiley & Sons Ltd, 2007.
31. Liu GR, Quek SS. *The finite element method: a practical course*. Oxford: Butterworth-Heinemann, 2003.
32. White RC, Limbert DA, Hederick JK, et al. *Guideway-suspension tradeoffs in rail vehicle systems, Report ERC-R-78035*. 1978.
33. Yang YN, Yau JD, Wu YS. *Vehicle-Bridge Interaction Dynamics*. World Scientific Publishing Co., Singapore, 2004.
34. Wilson SP, Harris NK, OBrien EJ. The use of Bayesian statistics to predict patterns of spatial repeatability. *J Transp Res Part C - Emerg Technol* 2006; 14: 303–315.
35. Dowling J, OBrien EJ, González A. Adaption of Cross Entropy optimisation to a dynamic bridge WIM calibration problem. *Eng Struct* 2012; 44: 13–22.
36. Quirke P, Cantero D, OBrien EJ, et al. Drive-by detection of railway track stiffness variation using in-service vehicles. *Proc Inst Mech Eng Part F J Rail Rapid Transit*, (Article in Press) (2016).
37. Esveld C. *Modern railway track*. 2nd ed. Delft: MRT-Productions, 2001.
38. Absi GN, Mahadevan S. Multi-fidelity approach to dynamics model calibration. *Mech Syst Signal Process* 2016; 189–206.